www.crt-journal.org

Crystal Research and Technology

Journal of Experimental and Industrial Crystallography
Zeitschrift für experimentelle und technische Kristallographie

WILEY-VCH

Cryst. Res. Technol. **46**, No. 5, 463 – 469 (2011) / **DOI** 10.1002/crat.201000213

Interplay between phase formation mechanisms and magnetism in the $Sr_2FeMoO_{6-\delta}$ metal-oxide compound

N. Kalanda*[1], S. Demyanov[1], W. Masselink[2], A. Mogilatenko[2], M. Chashnikova[2], N. Sobolev[3], and O. Fedosenko[1]

[1] Scientific-Practical Materials Research Centre of NAS of Belarus, 220072 Minsk, Belarus
[2] Department of Physics, Humboldt University Berlin, 12489 Berlin, Germany
[3] Departamento de Física and I3N, Universidade de Aveiro, 3810-193 Aveiro, Portugal

Received 5 April 2010, revised 20 March 2011, accepted 21 March 2011
Published online 1 April 2011

Key words double perovskites, strontium ferromolybdate, activation energy, precursors, macrograins textured, growth rate, mutual diffusion, crystallization mechanism, magnetization.

Double perovskites with the structural formula $A_2BB'O_{6\pm\delta}$, especially the strontium ferromolybdate $Sr_2FeMoO_{6-\delta}$, have attracted a lot of attention due to their unique magnetic and electrical properties and a possible application in spintronic devices. However, a strict correlation between the functional characteristics of $Sr_2FeMoO_{6-\delta}$ and its synthesis technology has been lacking up to date. Thus, we have studied in the present work the crystallization kinetics of $Sr_2FeMoO_{6-\delta}$ using reagents with different pre-history as well as the structural and magnetic properties of the obtained compounds. Differences in the crystallization kinetics as well as higher magnetic inhomogeneity of $Sr_2FeMoO_{6-\delta}$ synthesised from a mixture of MoO_3, Fe_2O_3, $SrCO_3$ in comparison with the compound synthesised from the $SrFeO_{2.5}$ and $SrMoO_{4-y}$ precursors have been found and interpreted.

1 Introduction

Solid solutions of transition metal oxides with double perovskite structure $A_2BB'O_{6\pm\delta}$ (A-alkali eath, B, B/ - heterovalent transition metals) have been intensely studied due to their unique magnetic and electrical properties [1-4]. Strong interplay between the electron spins, charges, and crystal lattice induces different electrical (conducting, semiconducting or isolating) and magnetic (para - (PM), antiferro- (AF), superparamagnetic (SPM) and ferrimagnetic (FRM)) states [5-8]. Possessing notable advantages as compared to manganites, complex transition metal oxides $A_2BB'O_6$ are very promising for spintronic devices [8,9]. In particular, strontium ferromolybdate $Sr_2FeMoO_{6-\delta}$ (SFMO) possesses high negative magnetoresistance (MR) of about 30% at 4.2 K, high Curie temperature of 400–430 K, nearly 100% spin polarisation, temperature stability of giant magnetoresistance (GMR), a chemical resistivity to reduction atmosphere and, therefore, reproducible magneto-transport characteristics [5,8,10]. Owing to a non-parallel arrangement of spins of the Fe^{3+} ($3d^5$; S = 5/2) and Mo^{5+} ($4d^1$; S = 1/2) cations that form an angle of 120°, generated ferrimagnetic structure determines the half-metallic state of the complex oxide with two separated conduction bands [11,12].

In SFMO the $3d^5$ electron shells of Fe^{3+} ($3d^5$; $t_{2g}^3e_g^2$) are fully occupied with spin-up $e\uparrow$ electrons. These electrons are located below the Fermi level and thus do not participate in the exchange interaction. On the contrary, the spin-down $t_{2g}\downarrow$ electrons of Mo^{5+} cations ($4d^1$; $t_{2g}^1\downarrow$) located within the conduction band at the Fermi level are mobile [13,14]. In this case, the mechanism of exchange interaction is realized by a double exchange of t_{2g} electrons located at the hybridized Fe($t_{2g\downarrow}$) and Mo($t_{2g\downarrow}$) orbitals of the Fe^{3+}($3d^5$; $t_{2g}^3e_g^2$) – O^{2-} ($2p^6$) – Mo^{5+}($4d^1$; $t_{2g}^1e_g^0$) chain group. This half-metallic nature of the electron states provides a nearly 100% spin polarisation in SFMO [15]. The theoretically predicted value of the magnetic moment in the double perovskite is about 4 μ_B per formula unit at T = 0 K. This value is higher than those obtained experimentally [16-18]. This discrepancy can be explained by the formation of antisite point defects, such as [Fe_{Mo}], [Mo_{Fe}], or of oxygen vacancies (V_0), as well as the appearance of structural inhomogeneities, e.g. magnetic clusters leading to the change of the type of exchange interactions is modified [19]. Therefore it is important to

* Corresponding author: e-mail: kalanda@physics.by

maintain the appropriate partial oxygen pressure taking into account the conditions of the synthesis. Our analysis of the results obtained by several authors revealed the multi-stage character of the crystallization of SFMO. This occurs due to the complex nature of the phase transformations, slow phase formation kinetics and low mobility of the $Fe^{3+}$and Mo^{5+} cations [20,21]. However, to the best of our knowledge, no strict correlations between the functional characteristics of the materials and their synthesis technology have been established. In order to fill this gap, we studied in the present work the crystallization kinetics of SFMO using reagents with different pre-history. Understanding of the correlation between the composition of the starting reagents and the physical and chemical properties of the obtained samples will pave the way to a precise control of the phase composition and Fe^{3+}/Mo^{5+}cation ordering in the strontium ferromolybdate. It has been found previously that during the SFMO growth the crystallization kinetics parameters depending on the relation between the kinetic and diffusional contributions to the process undergo constant changes. Therefore in this work we used experimentally determined, rather than theoretically obtained, chemical kinetics parameters.

2 Experimental

Two sets of starting reagents were used: (i) very high purity $SrCO_3$, Fe_2O_3, and MoO_3 oxides (Sample 1), and (ii) partially reduced $SrFeO_{2.5}$ (SFO) and $SrMoO_{4-y}$ (SMO) precursors (Sample 2). The complex oxides were obtained by the standard ceramic technology from MoO_3 and Fe_2O_3 oxides and strontium carbonate $SrCO_3$. Grinding and mixing of the stoichiometric blend of starting components were carried out for 3 h in ethyl alcohol in a vibromill. The obtained powders were dried at 350 K and then pressed into pellets. Upon the synthesis of the SFO and SMO precursors, the preliminary annealing was carried out for 20–40 h at 970 K and 1070 K, respectively. The final synthesis of the SFO and SMO compounds was performed in the Ar atmosphere at T = 1370 K for 20 h, and at 1470 K for 40 h in an Ar atmosphere, respectively, with the subsequent cooling down inside the furnace. The submicron size of the precursor grains (<d> ~ 200 nm) has been achieved by a prolonged (24 h) vibromilling in ethyl alcohol. The 4–5 mm thick pellets with a diameter of 10 mm, consisting of the starting reagents (MoO_3+0.5Fe_2O_3+2$SrCO_3$) or ($SrFeO_{2.5}$+$SrMoO_{4-y}$) and having a stoichiometric composition, were annealed in a polythermic regime at 300–1420 K and heating rates ϑ = 2, 7 and 15 K/min in evacuated quartz ampoules in the presence of a getter, with a subsequent quenching to room temperature. Both for the study of the superstructure ordering and for the magnetic measurements we chose two specimens selected among samples 1 and 2 that were annealed in a polythermic regime at 300 - 1420 K and a heating rate ϑ = 2 K/min in evacuated quartz ampoules in the presence of a getter with a subsequent quenching from 1420 K to room temperature.

The temperature in the furnace was measured using a Pt–Pt/Rh(10%) thermocouple and automatically stabilized within ±0.5 K. The phase composition of the solid-state synthesis products was determined by the X-ray diffraction (XRD) analysis using the CuK_α radiation in a DRON-3 diffractometer using the ICSD-PDF2 (Release 2000) database and the POWDERCELL software. The diffraction curves were measured at room temperature at the rate of 60 °/h in the angular range 2Θ = 15–70°. The transformation degree α i.e. the percentage of the material entered the SFMO synthesis reaction was estimated through the change of the normalized XRD reflex intensity $[I_{211}(112)/\{I_{211}(112)+I_{101}(112)\}]$ with temperature, where $I_{211}(112)$ and $I_{101}(112)$ are the maximum intensity reflexes corresponding to the SFMO and SMO phases, respectively. The magnetic properties of the samples were studied in a cryogenic vibrational sample magnetometer (VSM) in the temperature range from 4.2–300 K in magnetic fields up to 8 T.

3 Results and discussion

SFMO synthesis from the mixture of simple oxides occurs via a series of parallel and sequential phases [20,21]. In both samples, at the initial reaction stage the forming strontium ferromolybdate is enriched by iron, with the molybdenum content increasing in the course of the reaction. The molybdenum oxide in the ternary mixture reacts with the strontium carbonate somewhat more rapidly than the iron oxide does, except at the temperature T = 970 K, at which a practically simultaneous appearance of the XRD reflexes of the SFO and SFMO compounds is observed. The iron in the complex SFO oxide contained in the stoichiometric SFO + SMO mixture is more reactive at the formation of SFMO already at 870 K. Interestingly, the reaction rate $\beta = d\alpha/dt$ is higher in sample 2 synthesized from the SMO and SFO precursors than in sample 1 obtained from a stoichiometric mixture of Fe_2O_3, MoO_3, and $SrCO_3$, see (Fig. 1).

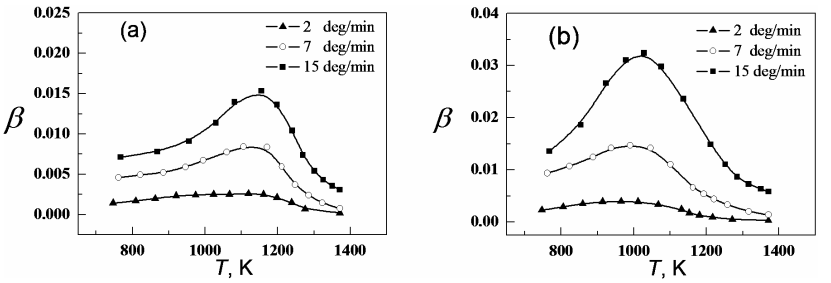

Fig. 1 Temperature dependences of the $Sr_2FeMoO_{6-\delta}$ growth rate in the samples synthesized (a) from a stoichiometric mixture of the MoO_3, Fe_2O_3, and $SrCO_3$ oxides – sample 1, and (b) from a mixture of the $SrFeO_{2.5}$ and $SrMoO_{4-y}$ precursors – sample 2. The corresponding heating rates are indicated in the panels.

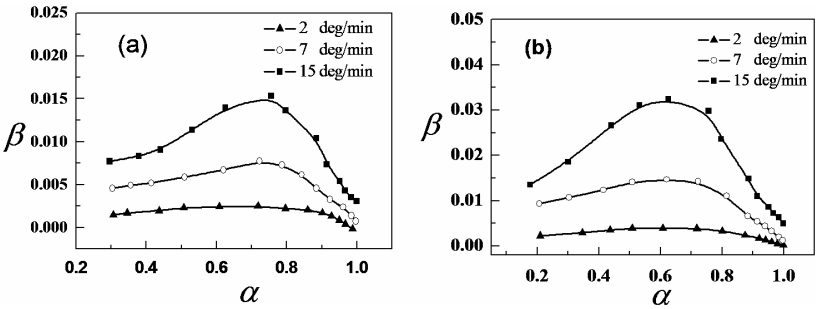

Fig. 2 The dependences of the $Sr_2FeMoO_{6-\delta}$ growth rate on the transformation degree in samples synthesized (a) from a stoichiometric mixture of MoO_3, Fe_2O_3, and $SrCO_3$ – sample 1, and (b) from a mixture of the $SrFeO_{2.5}$ and $SrMoO_{4-y}$ precursors – sample 2. The corresponding heating rates are indicated in the panels.

The fact that SMO and SFO enter the reaction more rapidly just at lower temperatures can be explained by increasing reaction surface area of the reagents. Nucleation of SFMO phase occurs on the strontium ferrite surface. Starting with the nuclei of the new phase, the phase interface penetrates into parental SFO phase, and the growth of the reaction product layer slows down the SFMO growth. If cations and anions in the product layer exhibit low mobility, then the heterogeneous reaction switches from the chemical adsorption type to the diffusional one, as indicated by the following results.

Staged variation of the SFMO crystallization rate has been found in the studies of the polythermic dependences of the reaction rate β of strontium ferromolybdate on the temperature, $\beta = f(T)_{\vartheta=const}$, and on the transformation degree, $\beta = f(\alpha)_{\vartheta=const}$, for fixed heating rates (ϑ = 2, 7, 15 deg/min) (see figures 1 and 2).

Increasing of the heating rate for both samples leads to an increase of the maximum value β_{max}. With increasing heating rate the $\beta_{max} = f(T)_{\vartheta=const}$ values shift toward higher temperatures, whereas $\beta_{max} = f(\alpha)_{\vartheta=const}$ stay practically constant, see table 1. The temperature at which the maximum reaction rate is attained is positively correlated with the heating rate. Degree of transformation is heating rate independent.

Table 1 Influence of the heating rate ϑ on the characteristic parameters T and α at which β is maximum.

Sample #	ϑ, deg/min	$T(\beta_{max})$, K	β_{max}	$\alpha\ (\beta_{max})$
	15	1150	0.015	0.6884
1	7	1146	0.008	0.7377
	2	1127	0.0024	0.7377
	15	1024	0.032	0.6241
2	7	993	0.015	0.6325
	2	964	0.0039	0.6333

It follows from table 1 that the chemical reaction rates are lower in sample 1 than in sample 2. Temperatures corresponding to the maximum values of β are 120–130 K higher than for the sample 1. Furthermore, the β_{max} values for sample 2 are by 0.10–0.15 higher than those for sample 1. From the analysis of the microstructure some difficulties of the crystallization of the strontium ferromolybdate in sample 1 were revealed. For instance, sample 1 possesses a less dense (average grain size <d> = 10 μm) and inhomogeneous microstructure, in which, beside the pores, elongated conglomerates, composed of densely packed grains with an average diameter of <d> = 3 μm and a length of up to 40 μm, are observed (Fig. 3). The presence of elongated conglomerates can be caused by the appearance of metastable phases with low melting temperatures, which leads to a local compaction and plastic flow. The porous structure of sample 1 may be generated by the emission of oxygen and carbon dioxide produced in the reaction between the components:

$$2\ SrCO_3 + 0.5\ Fe_2O_3 + MoO_3 = Sr_2FeMoO_{5.9} + 2\ CO_2\uparrow + 0.3\ O_2\uparrow.$$

A considerable reduction of the porosity in sample 2 with an average grain size of <d> = 2 μm may be caused by a lower amount of gases produced in the reaction:

$$SrFeO_{2.5} + SrMoO_{4-y} = Sr_2FeMoO_{5.9} + (0.3–y/2)O_2\uparrow,$$

and large agglomerates are absent due to the chemical homogeneity of the sample and to the presence of solid compounds with high melting temperatures (Fig. 4).

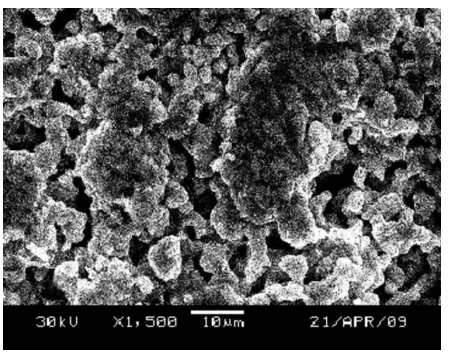

Fig. 3 Microstruture of sample 1 synthesized from a stoichiometric mixture of MoO_3, Fe_2O_3, and $SrCO_3$.

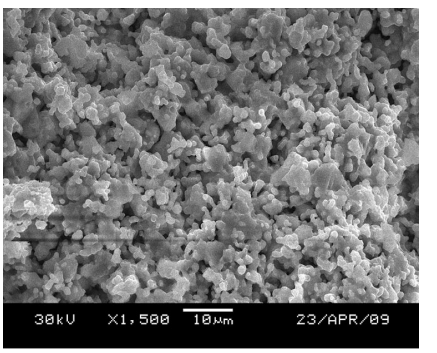

Fig. 4 Microstruture of sample 2 synthesized from a mixture of the $SrFeO_{2.5}$ and $SrMoO_{4-y}$ precursors.

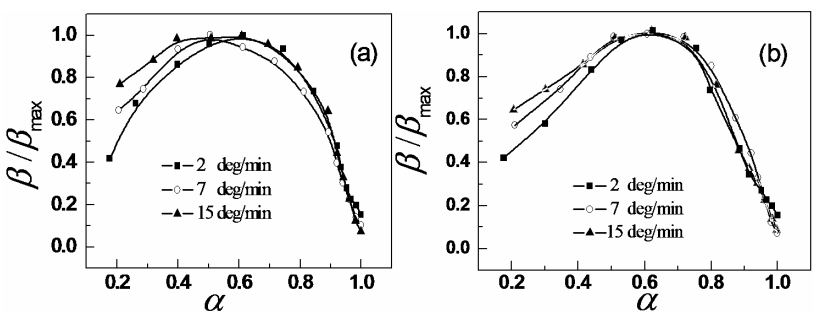

Fig. 5 Dependences of the relative transformation rate of $Sr_2FeMoO_{6-\delta}$ on transformation degree α for samples synthesized from a stoichiometric mixture of MoO_3, Fe_2O_3, and $SrCO_3$ – sample 1 (a), and from a mixture of the $SrFeO_{2.5}$ and $SrMoO_{4-y}$ precursors – sample 2 (b). The corresponding heating rates are indicated in the panels.

In order to determine the SFMO crystallization mechanism in samples 1 and 2, the obtained $\beta = f(\alpha)$ dependences were normalized to the maximum process rate β_{max} (Fig. 5 a,b). We have found that the $\beta/\beta_{max} = f(\alpha)$ curves are not homothetic in the interval $0.2 \le \alpha \le 1$. The maximum SFMO growth rate is achieved in sample 1 at various α values, whereas in sample 2 only at $\alpha \approx 0.61$.

Taking into account that (i) β values at $\alpha \ge 0.87$ for sample 1 and $\alpha \ge 0.92$ for sample 2 vary only insignificantly, (ii) $\alpha = f(T)$ dependence is governed by the process duration, and (iii) α depends on the heating rate upon the synthesis in the polythermic regime, it appears necessary to establish the intervals of α in which the SFMO growth occurs according to a certain mechanism. For this, the following boundary conditions have been introduced: $\gamma = 0$ at $\alpha = 0.2$ and $\gamma = 1$ at $\alpha = 0.87$ for sample 1; $\gamma = 0$ at $\alpha = 0.2$ and $\gamma = 1$ at $\alpha = 0.92$ for sample 2. It has been found that in sample 2 all kinetic curves $\beta/\beta_{max} = f(\gamma)$ turn out to be homothetic upon the use of the new normalized coordinates, which witnesses a unique SFMO crystallization mechanism in the interval $0.2 \le \alpha \le 0.92$ at a fixed heating rate (Fig. 6). It follows from the obtained results that a common behavior is inherent to both reaction blends investigated (samples 1 and 2), viz., a transition from the kinetic to the diffusion-limited regime, in which after the formation of a reaction product layer its blocking effect gets stronger with increasing layer thickness. However, in sample 1 the kinetic stage is a mixed one with the presence of a certain diffusion contribution caused by the formation of intermediate diffusion products, and the diffusion component increases as α grows. Assuming that in the diffusion-limited regime the reaction rate varies exponentially, $\beta \propto \exp(-E/kT)$, and in the kinetic one it behaves as a power of T, $\beta \sim T^n$, we can conclude that the increase of the β_{max} value in sample 2 occurs mainly due to the predominance of the kinetic regime. It is also indicated by homothetic character of the kinetic curves $\beta/\beta_{max} = f(\gamma)$ plotted in the new normalized coordinates, $\gamma = 0$ at $\alpha = 0.2$ and $\gamma = 1$ at $\alpha = 0.92$ (see above).

It has to be noted that the SFMO growth in sample 2 implicates various effects. So, the decrease of the oxygen content in $SrFeO_{3-x}$ facilitates the defect formation in the anion and cation sublattices of this compound

and, correspondingly, an increase in the diffusion mobility of cations during the synthesis of SFMO. The use of precursors increases the sample density, so that the diffusion length of the reagents towards the reaction zone is reduced, whereas the number of particles participating in the reaction is raised, thus enhancing the reaction capability of the reacting substances. The above mentioned reasons lead to an acceleration of the SFMO growth, lowering of the synthesis temperature, and appearance of superstructure ordering of the Fe^{3+} and Mo^{5+} cations in sample 2. The existence of superstructure ordering in sample 2 is confirmed by XRD spectra obtained on samples which were synthesized from a stoichiometric mixture of simple oxides and that of precursors (Fig. 7).

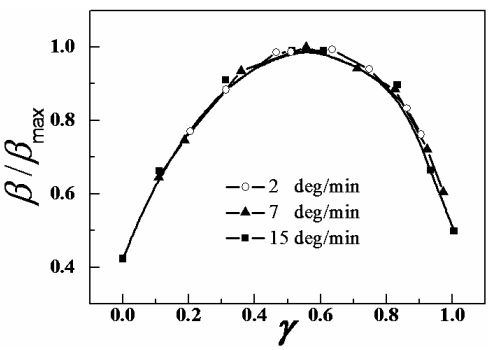

Fig. 6 Dependences of the relative transformation rate of $Sr_2FeMoO_{6-\delta}$ on γ for sample 2 synthesized from a mixture of the $SrFeO_{2.5}$ and $SrMoO_{4-y}$ precursors under consideration of the normalization conditions. The corresponding heating rates are indicated in the panel.

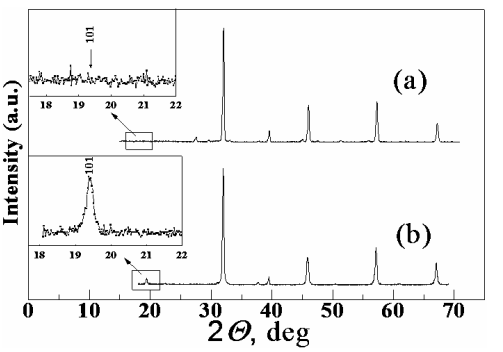

Fig. 7 XRD curves of $Sr_2FeMoO_{6-\delta}$ for samples synthesized from a stoichiometric mixture of MoO_3, Fe_2O_3, and $SrCO_3$ – sample 1 (a), and from a mixture of the $SrFeO_{2.5}$ and $SrMoO_{4-y}$ precursors – sample 2 (b).

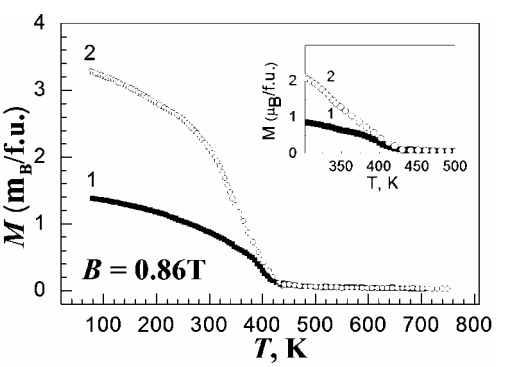

Fig. 8 Temperature dependence of the $Sr_2FeMoO_{6-\delta}$ magnetization for samples synthesized from a stoichiometric mixture of MoO_3, Fe_2O_3, and $SrCO_3$ – sample 1, and from a mixture of the $SrFeO_{2.5}$ and $SrMoO_{4-y}$ precursors – sample 2.

In order to study the influence of the prehistory of the starting reagents on the magnetic properties of samples 1 and 2, we have measured the temperature dependence of the magnetization (M) in the field B = 0.86 T. The Curie temperature of both samples was equal, $T_c \approx 418$ K. The magnetization of the sample 1 was $M(1)_{77K}$ = 1.33 μ_B/f.u., and for sample 2 we obtained $M(2)_{77K}$ = 3.07 μ_B/f.u., both values measured at T = 77 K. This means that the magnetization of the cation disordered sample 1 was 2.3 times lower than that of the dense sample 2 exhibiting a superstructure cation ordering (Fig. 8).

As the magnetic moment of the double perovskite SFMO is determined by the FRM ordering of the magnetic moments of $Fe^{3+}(3d^5)$ and $Mo^{5+}(4d^1)$ that form an angle of 120º, smaller $M(1)_{77K}$ values may be caused by the presence of magnetic clusters exhibiting AF coupling due to a disorder of the iron and molybdenum cations. A Fe^{3+} cation occupying a Mo^{5+} site is surrounded by Fe^{3+} cations, which leads to a change of the exchange interaction type and emergence of the Kramers-Anderson superexchange in Fe^{3+}–O^{2-}–Fe^{3+} and Mo^{5+}–O^{2-}–Mo^{5+} clusters with an antiparallel spin arrangement and a resulting lowering of the sample magnetization. The existence of 20–30 nm large magnetic clusters in similar samples has been formerly observed using low-angle neutron scattering [22]. The presence of AF clusters reduces the probability of forming a long-range FM order, which facilitates the fragmentation of FRM domains in smaller ones. The formation of a heterogeneous magnetic structure (AF–FRM) with a weak FRM coupling facilitates the implementation of a local paramagnetic state, in which the spin reversal does not change the energy of the AF–

FRM system, on the contrary to its magnetization. The inhomogeneous magnetic structure is facilitated by the porous microstructures of sample 1 that consists of weakly coupled grains of different sizes (Fig. 3). As a result, the magnetic phase transition of sample 1 in the vicinity of T_C is somewhat fuzzy, which may be interpreted as a manifestation of the PM state that is strongly affected by thermally activated fluctuations proportional to exp(–ΔE/kT). Furthermore, the presence of PM regions in samples 1 and 2 is indicated by measurements of the zero-field cooling (ZFC) and field cooling (FC) temperature dependences of the magnetization (Figs. 9, 10). It can be seen that, after switching on the field at 4.2 K, a steep magnetization increase upon the heating to 11 K is observed which amounts to 2.37% for sample 1 and 8.23% for sample 2. This witnesses the presence of regions with low coercivity. The latter is probably caused by the small size of the magnetic inclusions and their superparamagnetic character. Upon temperature increase from 4.2 to 280 K the $M_{ZFC}(T)$ dependence achieves a maximum at T_{max} = 180 K in sample 1 and at T_{max} = 265 K in sample 2. Above these temperatures, the samples exhibit a smooth transition from the AF–FRM into the PM state with blocking temperatures of T_B = 241 K and T_B = 305 K, respectively. Considering the temperature differences $\Delta T(\#1) = T_B - T_{max}$= 61 K and ΔT(#2) = 39 K, one can infer a higher magnetic heterogeneity of sample 1 than of sample 2.

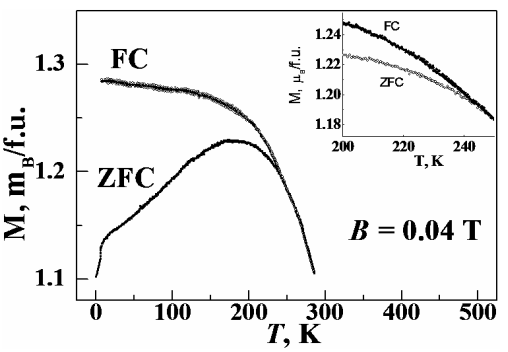

Fig. 9 Temperature dependences of the $Sr_2FeMoO_{6-\delta}$ magnetization for sample 1 synthesized from a stoichiometric mixture of MoO_3, Fe_2O_3, and $SrCO_3$ measured at B = 0.04 T in the field cooling (FC) and zero-field cooling (ZFC) regime.

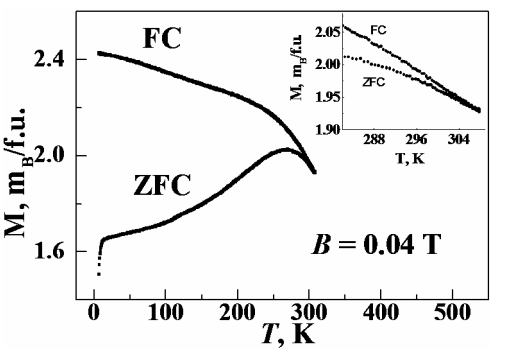

Fig. 10 Temperature dependences of the $Sr_2FeMoO_{6-\delta}$ magnetization for sample 2 synthesized from a mixture of the $SrFeO_{2.5}$ and $SrMoO_{4-y}$ precursors, measured at B = 0.04 T in the field cooling (FC) and zero-field cooling (ZFC) regime.

4 Conclusion

The obtained results demonstrate that for both reaction blends used, the one consisting of a mixture of the stoichiometric reagents MoO_3, Fe_2O_3, and $SrCO_3$ (Sample 1), and the other composed of the $SrFeO_{2.5}$ and $SrMoO_{4-y}$ precursors (Sample 2), a common behaviour is observed: there is a transition from the kinetic interaction regime to the diffusion-limited one, in which a formation of a reaction product layer is accompanied by an increase of its blocking action. It should be noted, however, that for the mixture of stoichiometric reagents MoO_3, Fe_2O_3, and $SrCO_3$ the kinetic stage of the solid-state reaction exhibits a mixed character involving a diffusion-limited component. Due to the formation of intermediate reaction products, and with the increasing transformation degree α, the contribution of the diffusion-limited component grows. The use of partially reduced $SrFeO_{2.5}$ and $SrMoO_{4-y}$ precursors consisting of submicron grains has allowed the synthesis of a single-phase $Sr_2FeMoO_{6-\delta}$ compound with a superstructure ordering of the Fe^{3+} and Mo^{5+} cations. In this synthesis mode, the kinetic difficulties of the $Sr_2FeMoO_{6-\delta}$ phase formation are largely reduced due to the increase of the diffusion mobility of the Fe^{3+} and Mo^{5+} cations and the shortening of their diffusion path into the reaction zone.

The analysis of the magnetization behaviour upon heating in a weak magnetic field of 0.04 T has revealed that in the temperature range from 4.2–11 K both samples contain magnetic regions with a low coercivity. The number of these regions is significantly higher in the high-density sample 2 than in the porous sample 1. The presence of nearly SPM regions explains the reduced magnetoresistance at T = 4.2 K. From the temperature differences $\Delta T(\#1) = T_B - T_{max}$= 61 K and ΔT(#2) = 39 K obtained from the temperature dependences of $M(1,2)_{ZFC}$ and $M(1,2)_{FC}$, one can infer a higher magnetic inhomogeneity of sample 1 synthesised from a

mixture of MoO_3, Fe_2O_3, and $SrCO_3$ in comparison with sample 2 synthesised from the $SrFeO_{2.5}$ and $SrMoO_{4-y}$ precursors and containing nearly uniformly sized grains.

Acknowledgements This work was supported by the ERASMUS-MUNDUS program, by Grant T09K-082 of Belarusian Foundation for Basic Research, and by project PTDC/FIS/72843/2006 of the FCT of Portugal.

References

[1] C. Frontera, D. Rubi, J. Navarro, J. L. Garcıa-Munoz, C. Ritter, and J. Fontcuberta, Physica B **350,** E 285 (2004).
[2] O. Chmaissem, B. Dabrowski, S. Kolesnik, S. Short, and J. D. Jorgensen, Phys. Rev. B **71** 174421 (2005).
[3] A. Pena, J. Gutierrez, L. M. Rodriguez-Martinez, J. M. Barandiaran, T. Hernandez, and T. Rojo, J. Mag. Mag. Mat. **254–255** 586 (2003).
[4] M. Sikora, O. Mathon, P. van der Linden J. M. Michalik, J. M. de Teresa, Cz. Kapusta, and S. Pascarelli, Phys. Rev. B **79**, 220402(R) (2009).
[5] S. E. Jacoboa, S. Duhalde, and R. C. Mercader, Physica B **354,** 59 (2004).
[6] T. Suominena, J. Raittilaa, T. Salminena, K. Schlesiera, J. Lindern, and P. Paturi, J. Mag. Mag. Mat. **309**, 278 (2007).
[7] D. Sanchez, J. A. Alonso, M. Garcia-Hernandez, M. J. Martinez-Lope, M. T. Casais, and J. L. Martinez, J. Mater. Chem. **13**, 1771 (2003).
[8] A. Poddar, R. N. Bhowmik, P. Muthuselvam, and N. Das, J. Appl. Phys. **106**, 073908 (2009).
[9] A. Rebello, V. B. Naik, and R. Mahendiran, J. Appl. Phys. **106**, 073905 (2009).
[10] Tian-Yi Cai and Zhen-Ya Li, J. Phys.: Condens. Matter **16**, 3737 (2004).
[11] O. Chmaissem, R. Kruk, B. Dabrowski, D. E. Brown, X. Xiong, S. Kolesnik, J. D. Jorgensen, and C. W. Kimbal, Phys. Rev. B **62,** 14197 (2000).
[12] M. K. Chung, P. J. Huang, W. H. Li, C. C. Yang, T. S. Chan, R. S. Liu, S. Y. Wu, and J. W. Lynn, Physica B **385–386,** 418 (2006).
[13] J. Linden, T. Yamamoto, M. Karppinen, and H. Yamauchi, Appl. Phys. Lett. **76**, 2925 (2000).
[14] D. D. Sarma, Solid State Mat. Sci. **5**, 261 (2001).
[15] K. I. Kobayashi, T. Kimura, H. Sawada, K. Terakura, and Y. Tokura, Nature **395**, 677 (1998).
[16] M. Itoh, I. Ohta, and Y. Inaguma, Mater. Sci. Eng. B **41**, 55 (1996).
[17] Y. Tomioka, T. Okuda, Y. Okimoto, R. Kumai, K.-I. Kobayashi, and Y. Tokura, Phys. Rev. B **61**, 422 (2000).
[18] L. Balcells, J. Navarro, M. Bibes, A. Roig, B. Martinez, and J. Fontcuberta, Appl. Phys. Lett. **78**, 781 (2001).
[19] T.-Y. Cai, Sheng Ju, and Zhen-Ya Li, J. Phys.: Condens. Matter **18**, 11347 (2006).
[20] T.-T. Fang, M. S. Wu, and T. F. Ko, J. Mat. Sci. Lett. **20**, 1609 (2001).
[21] T.-T. Fang and J.-Ch. Lin, J. Mat. Sci. **40**, 683 (2005).
[22] M. Watahiki, J. Susuki, Y. Tomioka, and Y. Tokura, J. Phys. Soc. Jpn. **70**, 67 (2001).

